An efficient method based on watershed and rule-based merging for segmentation of 3-D histo-pathological images

P.S. Umesh Adiga*, B.B. Chaudhuri

Computer Vision and Pattern Recognition Unit, Indian Statistical Institute, 203, B. T. Road, Calcutta-700 035, India

Received 19 August 1999; received in revised form 1 May 2000; accepted 1 May 2000

Abstract

This paper deals with the segmentation of 3-D histo-pathological images. Here we have presented a region-based segmentation method involving watershed algorithm and the rule-based merging technique. We have implemented a new method similar to flooding process for circumventing the inability to automatically mark the regional minima in small isolated objects. The 3-D histo-pathological images for testing the algorithm are obtained using confocal microscope in the form of a stack of optical sections. Normally, result of a classical watershed algorithm on grey-scale textured images such as tissue images is over-segmentation. We have proposed a rule-based heuristic merging technique to reduce the over-segmentation of cells. The tiny fragments of the cells and their parents are identified based on some heuristic rules and are merged together. Rule-based merging gives more than 90% accurate segmentation when compared to simple classical watershed extended to 3-D. Results are shown on 3-D images of prostate cancer tissue specimen.

Keywords: Histo-pathological; Watershed; Merging; Segmentation; Cell

1. Introduction

Automatic image analysis and decision making based on histological images is an interesting and non-trivial problem in histo-pathology. The difficulty in analysis of histo-pathological images arises due to closely clustered cells, which are touching or overlapping each other. Proper segmentation of these touching cells is key to automation of histo-pathological image processing. There exist as many segmentation techniques, as the segmentation problems. Even if the precise segmentation of the tissue image is achieved, inaccuracy in feature measurement persists due to usage of 2-D images. The two-dimensional images do not represent the complete cells in its entirety. Features such as size, shape, chromosome density, etc., cannot be measured precisely using 2-D images. Most of these problems can be reduced by the use of volumetric (3-D) images. Use of thick-tissue specimens and the three-dimensional (3-D) imaging results in complete and detailed representation of the cells. The study of spatial distribution of the cells, tissue architecture, tumor grading, structural and geometric feature measurements, counting of Fluorescence in situ Hybridization signals, etc., can be done more accurately by three-dimensional image analysis. Among recent developments in the visualisation of the histo-pathological images, Confocal Laser Scanning Microscopy (CLSM) is one of the most exciting new developments. Confocal microscope can be considered as a three-dimensional (3-D) imaging instrument for collecting data from spatial structures, especially biological ones. Relatively few works with practical biological results from such images have been presented. The use of quantitative study is even more recent [1,2].

The main hurdle in developing completely automatic image analysis tools for such 3-D histo-pathological images is the isolation of clustered and/or compactly arranged cells. The edge operators such as Marr-Hilderth

[3], Canny edge detector [4], etc., may not segment the cells completely due to low and uneven gradient magnitude where the cells touch one another or overlap. Moreover, marking edges or boundary does not complete the process of segmentation. The edge-based segmentation is prone to problems such as marking of noisy edges, discontinuous boundary, etc. [5]. On the other-hand, region-based techniques i.e., isolation of the different regions in the image is more suitable for tissue segmentation. This technique stems from the fact that the voxels belonging to the same region show many similar characteristics. Most simple and primitive region-based technique is thresholding the image based on local histogram of the voxel intensity and then labelling the isolated regions by connected component-labelling algorithm [6,7].

When the objects are well isolated, thresholding and labelling process may give acceptable results. But, rarely real-life images show uniform grey level within the object as well as in the background. Moreover, histogram-based thresholding does not exploit the fact that the points from the same object are generally, spatially close due to the surface coherence [8]. Techniques such as split and merge algorithm [9], simple region growing [10], multiple thresholding [11], etc., do not produce acceptable segmentation results due to the fine textured nature of the cell chromatin and the presence of dense intracellular as well as intercellular matters. In our previous article [2], we have described an edge-based segmentation method for CLSM images and its application in confirming the membership of a FISH signal to a corresponding cell nucleus. In this paper we have described a special type of region growing method, which is popularly known as watershed algorithm that gives acceptable results in most of the cases. The technique is extended to work on 3-D tissue images. Watershed technique is suitably modified to avoid the problem of automatic marking of regional minima. We have also presented a methodology to correct the over-segmentation, which characterises the segmentation of tissue images using watershed techniques.

Segmentation based on the use of watershed lines to separate the regions has been originally developed in the framework of mathematical morphology [12,13]. When we map the grey-scale image as a topographic surface, the topography can be viewed as watersheds. The grey level of each voxel stands for the elevations of the corresponding watershed surface. Though mapping of grey levels, as a topographical relief in three-dimensional image is more ambiguous to visualize, the algorithm is a simple extension of two-dimensional watershed to 3-D with a modified region growing. Watershed algorithms were extensively used for segmentation of 2-D histo-pathological images. Some of the important works in this regard are of Beucher [12], Beucher and Meyer [13], Vincent [14], Lockett and Herman [15], Najman and Schmitt [16], Malpica et al. [17], etc.

2. Segmentation: a 3-D watershed approach

Segmentation of 3-D histo-pathological images can be considered as good iff the results show the following properties.

(1) Complete and detailed isolation of the clustered cells.
(2) Minimum over-segmentation and under-segmentation of the cells.
(3) Each visually perceivable 3-D cell region has been given a unique label.
(4) The segmentation process should be less interactive and the results should be comparable to manually segmented results. The process should be fast and efficient considering the large size of the volumetric data sets.

Classical watershed algorithm partially satisfies all these conditions. Though it is said that mostly all the cells are separated at the end of watershed algorithm application, more often, a single cell is divided into several fragments resulting in over-segmentation. This results in labelling the parts of the same cell as different individuals. There are few methods suggested in the past literature to overcome this problem [12,13,16]. The histo-pathological images are often noisy and the cells we want to segment are often complex and varied in its shape, size or intensity. When we look at the result of a watershed segmentation of a histo-pathological image, we find that most of the cells are fragmented. Merging the fragments of the same cell into a single object may produce desired results. In this paper along with explaining the practical implementation of watershed in 3-D, we have presented a rule-based merging algorithm to reduce the over-segmentation. To a major extent, one can reduce the over-segmentation by undertaking proper noise reduction and feature enhancement of the objects of interest in the image before applying segmentation techniques. We have used few pre-processing techniques to achieve the same. These techniques are briefly described below.

2.1. Pre-processing

Separation of image background and foreground regions not only defines a broad area of interest but also reduces ambiguity in the results due to uneven and dense background. As it is well known and we can see later in our experimental results too, noise and other artefacts present in the image results in the over-segmentation of the cells and the tissue. Several conventional and heuristic methods are therefore necessary to reduce these artefacts in the image. We have implemented a simple window-slicing method to achieve this. Window slicing, which is also known as amplitude thresholding, converts all the pixels or voxels, which are below a threshold T, to the lowest grey value that is zero (indicating dark

background). The voxels having intensity value above the threshold is kept undisturbed. This gives us an image of uniform background while the foreground consists of different grey levels. We have observed that the histogram of our image data sets exhibits unimodal property. Hence, the valley point indicating likely threshold, may not be found explicitly in the histogram of the images. In such cases it is often possible to define a good threshold at the *shoulder* of a histogram [18]. There are several methods to choose the shoulder point of the histogram. We have used an empirical formula, $\tau = (\mu \pm k\sigma)$ where σ is the standard deviation and μ is the average grey value and k is a constant determined as follows. The difference in the number of voxels in foreground for $(\mu \pm k\sigma)$ and $(\mu \pm (k+2)\sigma)$ is calculated. If this difference is small (approximately $\leqslant 10\%$ of the total number of foreground voxels calculated as per $(\mu \pm k\sigma)$), then corresponding value of k is considered as the constant for threshold selection. We begin this iterative process of determining k with $k = 0$ and increase k by 1 till the said condition is satisfied. Here, $\tau = (\mu + k\sigma)$ when the mode point of the histogram lies close to the minimum grey value in the image and $\tau = (\mu - k\sigma)$ when the mode point lies close to the maximum grey value in the image. Sometimes, window slicing results in creation of holes in the cells and small noisy island-like structures in the background. This is due to the presence of dense non-cellular matters in the background and dark intra-cellular objects within the cell. We have developed a size- and shape-heuristic-based filter to reduce this effect.

The size of all the isolated objects is calculated. If the size is less than pre-defined size threshold then such an object is considered as artifact and its voxel intensity are changed to background intensity. Similarly, the holes are identified. If the holes are smaller than the pre-defined threshold, then the original grey values of the voxels belonging to the holes are restored. Figs. 1(b) and (c) show the result of window slicing and size filtering on a representative image slice of CLSM image stack. The representative image slice is shown in Fig. 1(a). After window slicing and size filtering of the image stack, the background noise is reduced and the background grey value becomes spatially uniform.

The main problem with the confocal image stack is the attenuation of light along the depth of the specimen. The uneven illumination along the depth of the specimen results in the spatial variation of light intensity in the image volume. Besides the optical problems, the photo-bleaching of the specimen contributes to the degradation of intensity. Photo-bleaching can be modelled as a first-order decay process and hence computationally corrected [19]. When we plot the average image intensity of each image slice against depth of the stack, we have observed that the illumination degradation is not linear. We have implemented a simple method of restoration of intensity of the foreground voxels by comparing it with

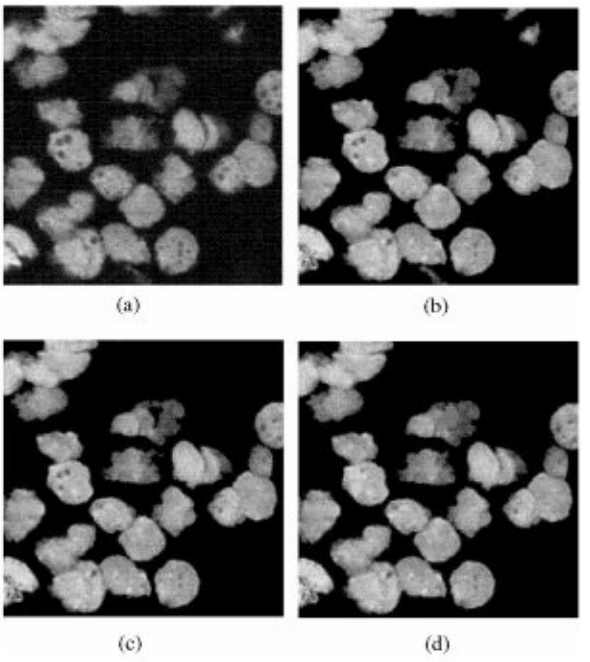

Fig. 1. Result of image enhancement steps shown over a single image slice: (a) original image slice, (b) result of window slicing, (c) result of size-filtering, (d) result of morphological opening and closing of a 3-D image.

the highest intensity image slice in the stack. Let I_i be the image slice having maximum average image intensity, i.e., $I_i = \max\{I_1, I_2, \ldots, I_n\}$ where $I_1, I_2, \ldots, I_n$ are the intensities of $(1, 2, \ldots, n)$th image slice in the stack. We consider this image slice i as the standard image slice and increase the average image intensity of remaining image slices in the stack to be on par with average image intensity of image slice i. Increasing the average image intensity of the whole image slice increases the background intensity too, which is undesirable. Hence, we have to consider only those voxels that belong to a particular region of interest where the intensity restoration is necessary. The foreground (highlighted by locally high grey value or image intensity due to specific fluorescent material) of the image is considered as the region of interest in the present case. Such a region is readily available from the results of window-slicing and size-filtering.

Let the mean intensities of the image slices $1, 2, \ldots, n$, in the image stack be $\bar{I}_1, \bar{I}_2, \ldots, \bar{I}_n$. The variation in the average image intensity of the foreground is plotted as shown in Fig. 2. If $\bar{I}_i$ is the average intensity of reference image slice, such that $\bar{I}_i \geqslant \bar{I}_j$ for all j, then, image slice i is considered as the reference image slice and $\bar{I}_i$ as the standard image intensity value. Let $\beta_k = |\bar{I}_i - \bar{I}_k|$ be the difference of average intensity of the foreground in kth

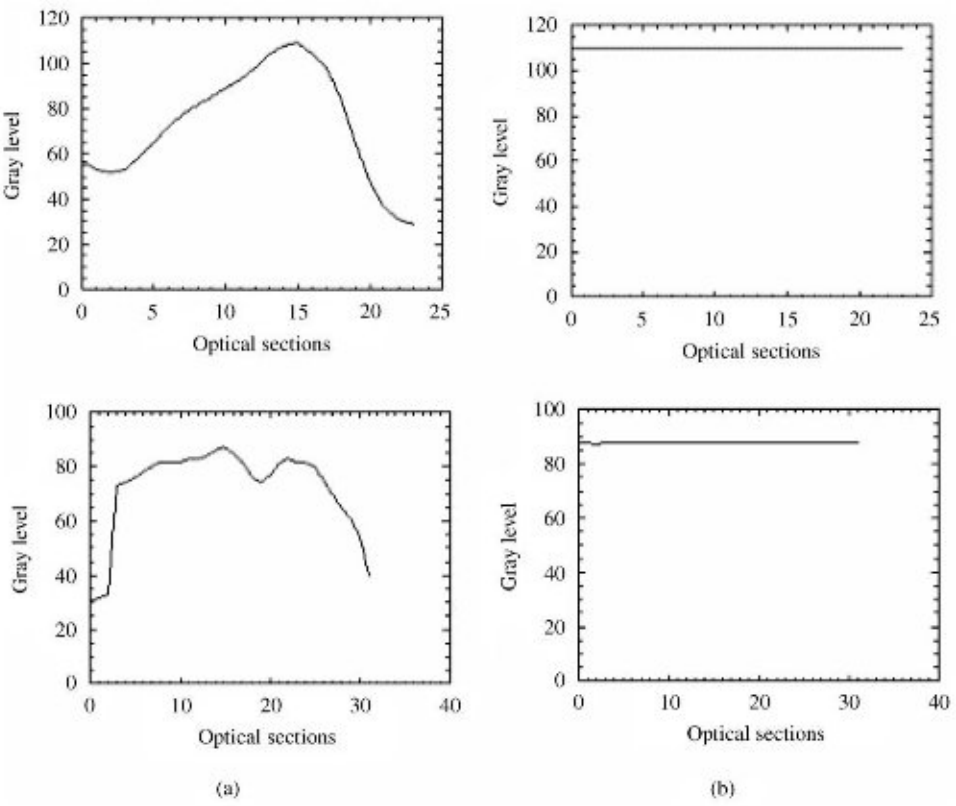

Fig. 2. Variation of average image intensity of the foreground (a) before restoration and (b) after restoration.

image slice and the reference image slice i. Then for the kth image slice the grey level of each pixel of the foreground is enhanced by a factor $c\beta_k$, i.e., if $I(x, y, k)$ is the intensity of voxel at (x, y, k) then the enhanced intensity is given as $I(x, y, k) = I(x, y, k) + c\beta_k$ where c is an experimentally chosen constant. Ideally c should be 1. This simple addition of the average value to the image intensity results in the loss of pixel sensitivity. A trade-off optimising the requirements of light intensity and loss of sensitivity is useful. This trade-off is also imaging and application dependent. As the confocal microscopy images do not give clear details of the intra-cellular structures as well as our interest being limited to measure the quantitative features of cells and the tissue, we have ignored the pixel sensitivity issue. One can use simple contrast stretching operation [20] to enhance the visual quality of the intensity restored image.

One of the major reasons identified for over-segmentation or wrong segmentation results in watershed algorithm is the presence of holes inside the object and the barb-like structures at the object surface. These artefacts can be reduced by the application of morphological operators. Morphological opening and closing operations break the narrow isthmuses and eliminates small islands and sharp peaks. This is very important as the removal of noisy peaks and islands result in more accurate construction of geodesic distance map, which holds the key to reduce the over-segmentation. Opening of an image $I(x, y, z)$ by a structuring element K is denoted by $I(x, y, z) \circ K$ and defined as $I(x, y, z) \circ K = (I(x, y, k) \Theta K) \oplus K$. The closing of the image by the same structuring element can be defined as $I(x, y, k) \bullet K = (I(x, y, k) \oplus K) \Theta K$, where Θ is the erosion operator and $\oplus$ is the dilation operator [21]. We have used three-dimensional $3 \times 3 \times 3$ six connected structuring element for this purpose. Fig. 1(d) shows the result of morphological opening and closing on a 3-D image.

2.2. Watershed algorithm

Segmentation by watersheds was first proposed by Lantuejoul [22], and was later improved jointly with Beucher [23]. Classical watershed algorithm can be categorized as a region growing process. Briefly stating, each cell is assigned a regional marker approximately at the center of the cell. A voxel in the foreground is clubbed with a nearest regional marker if its geodesic distance from the corresponding regional marker is less than its

geodesic distance from any other regional markers. When the regional minima or markers are completely grown, they approximately represent the region of a single cell separated by different labels assigned to regional markers or by those voxels whose geodesic distance is the same for more than one regional marker. Before going to implementation details and the improvement of the watershed algorithm, we have described few standard terms used in watershed paradigm namely, regional minima, zone of influence, SKIZ, watershed lines, etc., concerning 3-D objects to be segmented.

The regional minima R_i of a 3-D object is defined as a connected group of voxels at the approximate center of the object characterised by the following property. If the shortest distance of this group of connected voxels from the object boundary is d_i, then it is not possible to traverse to another region of distance longer than d_i without traversing through the voxels of distance value shorter than d_i. In simple words, a regional minimum is a group of voxels or a single voxel, belonging to the object and has a maximum distance value from the nearest background voxel than other voxels in the object. Fig. 3 shows the concept of regional minima with respect to a 3-D object.

The geodesic distance d_i of a voxel i from the regional minima R_i of a 3-D object in a spatial image domain is the length of a shortest existing path within the foreground and linking voxel i and regional minimum R of the object. Fig. 3 presents the concept of geodesic distance. The *zone of influence* (ZOI) of a regional minima R_i consists of all those voxels whose geodesic distance d_i from the regional minima R_i is smaller than their geodesic distance to all other regional minima $R_{j\neq i}$ where $j = 1, 2, \ldots, N$, N being the total number of regional minima in the image volume. Fig. 3 shows the concept of zone of influence diagrammatically. The zone of influence of each cell marker (regional minima) approximately covers the voxels belonging to the respective cells. The ZOI are also called as catchment basins.

One of the simple methods to find the regional minimum is to appropriately threshold the distance map such that each cell gets one regional marker. For defining the accurate zone of influence of each regional marker, Euclidean distance of all the voxels from the nearest regional marker should be calculated to define the ZOI of each regional minimum. Calculation of accurate Euclidean distance for each foreground voxel from the nearest regional minima is computationally expensive. A very close approximation to Euclidean map can be used to define the zone of influence of the each regional marker. We have used path generated distance transforms (PGDT) as proposed by the Borgefors [24] for finding the zone of influence.

Two-tone version of the image is obtained by thresholding the image at suitable level as explained earlier. All the background voxels are given a distance value 0

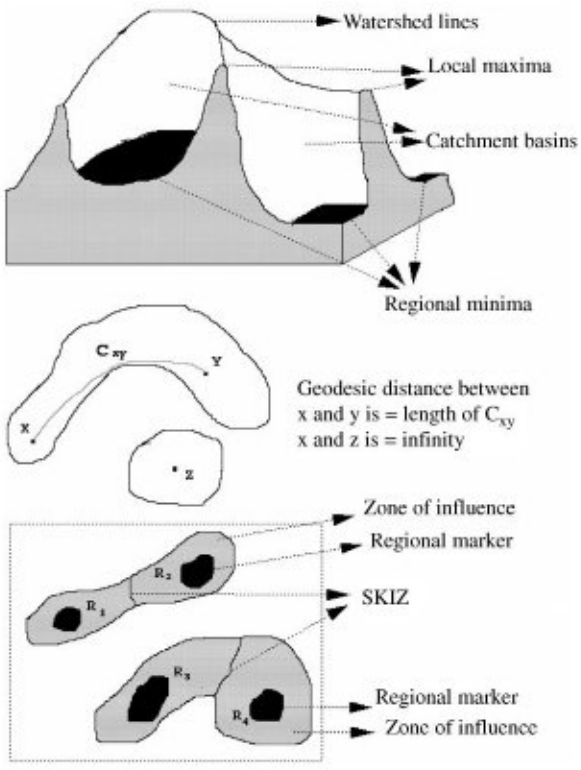

Fig. 3. Diagrammatic description of several terms used in watershed paradigm.

while the foreground voxels are given a very high distance value (ideally infinity). In the first scan from the top-left, a new distance value is computed for the foreground voxel. A $3\times3\times3$ neighbourhood of each foreground voxel is considered along the raster scan. Compute the sums of the values of the already visited neighbours and the corresponding local distances. In 26 neighbourhoods there are 13 already visited voxels for each central voxel. Thus, the new distance value for the central voxel is the minimum of the 13 sums. This scan computes the distances from the left-up-top. In the second scan, the scan direction is reversed. Again for each voxel, sum of the already visited neighbour distance values and local distances are computed. The only difference is that now the central voxel itself must be included, adding local distance zero. Thus the new, final value is the minimum of the 14 sums. The second scan computes the distances from right-down-bottom. Local distance of [3,4,5] is given to a [face-connected, edge-connected and comer-connected neighbourhoods] in a 26 neighbourhood voxel lattice.

The skeleton by zone of influence (SKIZ) is defined as the surface consisting of those voxels in the foreground which do not fall into ZOI of any particular regional

minima R_i where $i = 1, 2, \ldots, N$. Voxels of SKIZ surface would have the same geodesic distance from more than one regional marker. This SKIZ surface forms the *watershed lines* separating the zone of influence of different regional minima.

Explanation about some other related terms such as sinks, divides, channels, hills, ridges, ruts, etc., of a function can be found in Ref. [25]. With the knowledge of these terms used in watershed paradigm, we will be able to explain how this methodology can be used to segment the 3-D cells in a thick-tissue section images.

2.2.1. Segmentation

Enhanced and window-sliced image stack is converted to two-tone image by changing all the foreground voxel values to 1 and the background is kept the same i.e., zero. This two-tone volumetric image is used to calculate the geodesic distance map as explained earlier. The distance map is then suitably thresholded such that maximum number of cells would have a signature in the thresholded distance map. These regions in the thresholded map are superposed on the distance map as regional markers. When all the cells in the image are more or less of similar size and shape, thresholding a distance map results in a regional marker for every cell in the tissue. Unfortunately, that is not the case with the data sets we are working on. One way to circumvent this is to find the marker by successive erosion. In successive erosion, the two-tone version of the image is successively eroded with a suitable structuring element. Care should be taken so that no cell signature is completely eroded from the image domain. This can be done by setting a size threshold and not to erode any cell signature that is smaller than the size threshold. The eroded cell signatures are then considered as regional markers and the ZOI of each marker can then be calculated by generating a suitable distance map. In some cases it is found that successive erosion results in more than one regional marker for each cell. This results in over-segmentation. We have used thresholded distance map for marking the regional minima and those cells which do not have regional minimum marked in them are taken care of during the region growing process which is explained below. Each regional minima obtained from thresholding the distance map is given a unique label by using a 3-D component labelling algorithm and the results are kept separate [2].

The regional minima R_i is grown into its neighbourhood voxel v_i iff the geodesic distance from R_i is less than the distance from any other regional marker. Small isolated or touching cells that do not have any regional minima will be lost if we just concentrate on growing the regional markers into their neighbourhood. We have used voxel merging rather than region growing to circumvent this problem. Here all the voxels having a distance value d is merged with the neighbouring regional marker or if there is no regional marker within a finite geodesic distance (neighbourhood), the voxel is merged with a higher distance value voxel in its immediate 26 neighbourhoods or the voxel itself becomes a new regional marker. The following algorithm explains this.

The process of 3-D watershed segmentation can be explained in a few steps. Let R_i for $i = 1, 2, 3, \ldots, N$, be the labelled regional markers where N gives the maximum number of regional markers in the image. Let $dist(.)$ represents the distance value of voxels or regions in the distance map.

Step 1: All the regional markers are given maximum distance value within the image domain i.e., $dist(R_j) = \max\{dist(v_i)\}$ for all i and j. Let $d_{\max}$ be the maximum distance or the distance value of the regional markers.

Step 2: Then, all the voxels having a distance value $(d_{\max} - 1)$ and located in the neighbourhood of a regional marker are merged with their nearest regional marker. The merging process can be said as the growing of the labelled regional markers into the neighbourhood voxels, which falls into its zone of influence.

Step 3: The isolated voxel or group of connected voxels with distance $(d_{\max} - 1)$ and not having a labelled regional marker in their immediate neighbourhood are given a new label and considered as new regional markers and given a new unique label. This also shows that, one can start with a single voxel of highest distance as the only regional marker and still be able to segment all the regions in a cluster of objects.

Step 4: $d_{\max} = d_{\max} - 1$.

Step 5: If the $d_{\max} \neq 0$ then steps 2–4 are repeated.

This process of region merging for growing the regional marker takes care of those cells, which are not marked with regional markers initially. The process of voxel merging stops when all the voxels in the foreground is merged with a nearest regional marker or merged to a highest distance value within the region when regional marker is not found. The result of watershed-technique-based segmentation is usually fragmentation of the cells in the image. Here we propose a region merging technique as a post-processing algorithm to reduce the over-segmentation of the cells.

3. Rule-based merging of the over-segmented cells

In histo-pathological images, inside of the nuclei is a texture chromatin and the outside is a cytoplasm, which is also textured. The texture variation is so dominant that it makes it difficult to discriminate between the contour lines of the cell and the chromatin texture patterns. If we construct the watershed lines directly from such a textured image, it results in a severe over-segmentation as shown in Fig. 4(b). Fig. 4(a) shows the un-

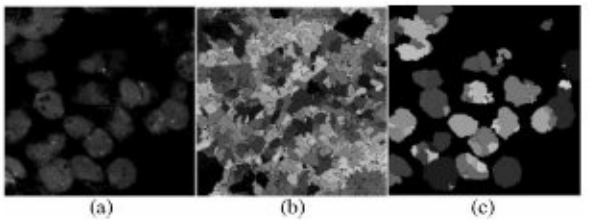

Fig. 4. Result of simple watershed technique shown over a single image slice: (a) original image slice, (b) result of watershed segmentation considering the grey-level topography of the image for marking different regions, (c) result of watershed considering distance map to mark different regions.

processed image slice. The segmentation of the cells by the direct construction of the watershed lines based on grey-level topography results in too many fragments. This is due to the fact that every regional minimum becomes the centre of a catchment basin, i.e. every regional minimum is considered as belonging to a unique cell and its ZOI is calculated. Even if we use the enhanced and window sliced image for the application of watershed algorithm, some over-segmentation persists as is evident from Fig. 4(c). When we automatically choose the regional marker by thresholding the distance map, there is every possibility that the same cell may get more than one regional minimum. Successive erosion also results in more than one marker seed per cell. The holes and the sharp protrusions which appear inside the thresholded image for calculating the distance map which are not cleaned during pre-processing results in wrong calculation of the distance map and hence results in more than one regional marker within the same cell.

Several researchers have tried to address this problem [13,16,26]. One possible method is to make use of hysterisis thresholding to suppress the noisy, weak contours, representing the watershed lines between small regions. Najman and Schmitt [16], have listed various reasons for ill suitability of hysterisis thresholding in case of watershed. They are: (1) Hysterisis thresholding is suitable for edges and it produces non-closed contours while watershed contours are already closed contours, which are obtained as a complimentary to the set of regions. (2) Hysterisis thresholding on watershed segmentation produces barbs, etc. Some of the proposed method to overcome the over segmentation problem is the geodesic reconstruction [12], the hierarchical segmentation [13], hierarchical segmentation using dynamics of contour [16], etc. We have proposed an extension to 3-D watershed technique, which identifies the over-segmented objects based on simple size and shape features and merge them with their parent cell.

Let N be the total number of segmented objects due to the application of simple 3-D watershed segmentation method. Let N be the total number of segmented objects due to the application of classical 3-D watershed segmentation method. Let T_{size} be the size threshold for a cell, i.e. a cell should have a minimum size of T_{size}. This threshold is set experimentally. All the tiny fragments of the cells whose sizes are below T_{size} are considered as noisy and are merged with corresponding parent cell. We assign fragment 'a' to a parent cell 'A', if the following heuristic conditions hold good.

1. 'A' and 'a' should be touching neighbours, $size(A) > size(a)$ and $size(a) \leqslant T_{size}$.

2. If 'a' is sharing its boundary with more than one large cell fragment, then the length of the boundary it shares with 'A' should be larger than the length of the boundary it shares with any other touching large object.

If these conditions are satisfied then the fragment 'a' is merged with the parent cell 'A'. To reduce the possible errors due to group of tiny fragments being sandwich between two large objects, we merge those fragments first which are touching neighbours to large objects. Also, after merging one fragment to a large object, merging of

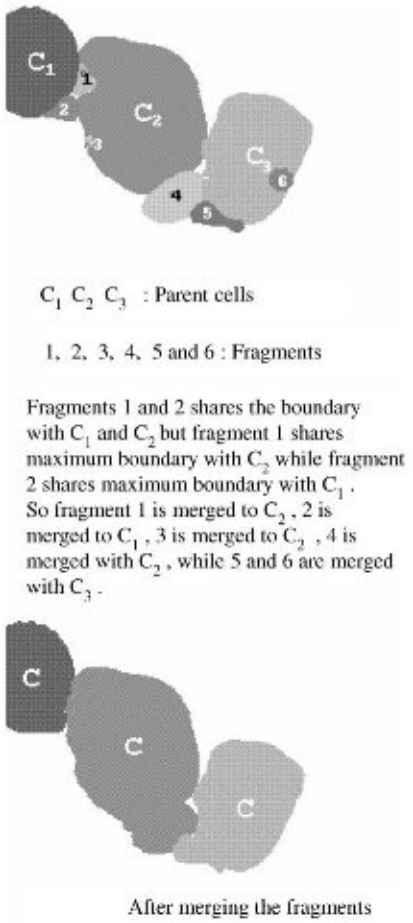

Fig. 5. Diagrammatic representation of detecting the small fragments of the object and finding its parent.

any other small object to the same large object is considered only after all the other large objects are checked for merging possible single fragment. Fig. 5 diagrammatically explains the detection of fragments and their parental cells.

When fragment '*a*' does not have any large touching neighbour but has many small fragments as its neighbours, then there is a possibility that a single cell might have been over-segmented to such a level that there is no fragment of size above threshold T_{size} belonging to that cell. In such cases, all the tiny fragments that are touching each other and not connected to a larger object, are merged to form a single object. If this merged object is above the threshold T_{size} then it is considered as a cell otherwise it is discarded as a noise artifact. The merging process stops when all the tiny fragments are either merged with a larger object or are discarded considering them as artefacts.

Fig. 6(a) shows a sequence of image slices of a 3-D image stack while Fig. 6(b) shows the result of a classical watershed algorithm extended to 3-D. Fig. 6(c), shows the result of automatic rule-based merging of the small objects in the over-segmented image volume. There can be still many cases where large individual cells are found to be segmented into two or three different objects. This may be due to the fact that such artefacts do not fall into the size threshold chosen by trial and error methods. Moreover, the rule-based merging is not foolproof as it is based on heuristic assumptions.

4. Experimental results and discussions

A Silicon Graphics, Indy machine with IRIX 5.3 is used as a platform to run the software. Much of the programming is done using Interactive Data Language

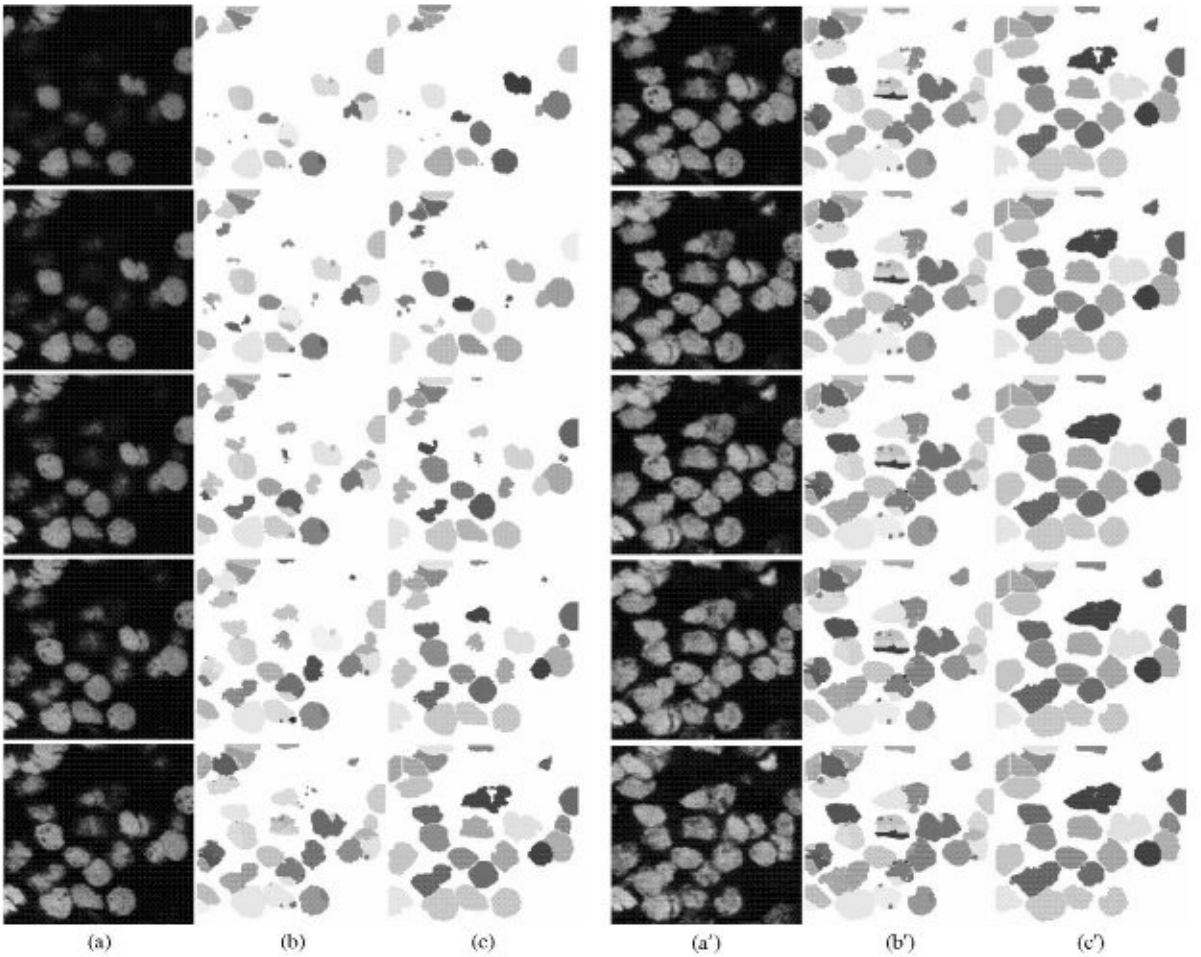

Fig. 6. Result of 3-D watershed technique shown over a sequence of image slices of a 3-D stack: (a, a') original image slices, (b, b') result of classical watershed extended to 3-D, (c, c') result of classical watershed with a rule based merging.

Table 1
Comparative result of cell region isolation by simple 3-D watershed, watershed with selective marker technique, and watershed with rule-based merging

Sl. no.	Actual number of cells present	Number of cells by simple 3-D watershed	Number of cells by selective marker technique	Number of cells by rule-based merging technique
01	23	42	24	24
02	31	56	31	32
03	18	29	23	21
04	42	67	47	38
05	26	38	29	26
06	12	19	12	12
07	05	05	05	05
08	31	49	34	33
09	28	43	31	31
10	37	56	42	40
11	11	11	12	13
12	12	12	12	12
13	16	21	18	17
14	28	44	30	31
15	07	09	07	08
		%error = 53%	%error = 9%	%error = 2%

(IDL) and C. Most of the experiments needed no human interactions except to load the images.

Fig. 6 shows the results of the segmentation presented in this paper. The 3-D watershed technique with rule-based merging has taken 1 min 20 s with 95% correct segmentation of cells in a image of size $256 \times 256 \times 24$ consisting of 22 cells of different size and shape. Without rule-based merging, results can be obtained within a minute but the segmentation is found to be only 53% correct. These figures are mentioned with respect to a particular data set. Though for a reliable statistical evaluation, one has to experiment on large amount of data before deciding the efficiency of a particular methodology, the above result is definitely an indicator of the utility of rule-based merging. Rule-based merging allows us to do away with selective regional minima marking or hysterisis thresholding to reduce the over-segmentation.

Table 1 gives comparative results of simple 3-D watershed, watershed with a selective marker technique [13] and watershed with rule-based merging technique as applied to the segmentation of 3-D cells. Quantitative results are shown on 15 3-D image data set of a prostate cancer tissue. From this table it is evident that classical 3-D watershed is of very little use for segmentation of 3-D histo-pathological images unless some additional technique is used to reduce the over-segmentation.

The three-dimensional extension of watershed algorithm is quite similar to the 2-D counterpart extensively used for segmentation. The 3-D neighbourhood relation and its equivalent distance calculation enhance the complexity of the overall process. Presence of noise or hidden holes in the 3-D objects makes the segmentation a difficult process especially the use of watershed technique. Extensive pre-processing of the 3-D images is necessary to avoid the over-segmentation. An evolving approach for marking the regional minima in the technique presented in this paper reduces the problems due to improper marking of regional minima. Given a correct geodesic distance map, proper region isolation can be assured by using this technique.

In the future work, we plan to study the influence of different region-based segmentation techniques on the measurement of important cytological and histological features. We also plan to combine these techniques to produce better segmentation results.

Acknowledgements

We would like to thank all the scientists of Biomedical Image Analysis Division, Institute of Pathology, GSF, Munich, Germany for providing the data sets. Special thanks to Mr. Rodenacker and Dr. Umapada Pal for introducing us to watershed techniques. The work was partly supported under the project Indo-German collaboration of Bio-medical research sponsored by International Beuro, Germany and ICMR, India. We thank both the organisations for their support.

References

[1] R.S. Acharya, C.J. Cogswell, D.B. Goldgof (Eds.), Biomedical Image Processing and Three-dimensional Microscopy, SPIE Proceedings, Vol. 1660, SPIE Press, Bellingham, USA, 1992.

[2] P.S.U. Adiga, B.B. Chaudhuri, An efficient cell segmentation tool for confocal microscopy tissue images for quantitative evaluation of FISH signals, J. Microsc. Res. Tech. 44 (1999) 49–68.
[3] D. Marr, E. Hilderth, Theory of edge detection, Proc. Roy. Soc. London B 207 (1980) 187–217.
[4] J. Canny, A computational approach to edge detection, EFEE Trans. Pattern Anal. Mach. Intell. 8 (1986) 679–698.
[5] C. Garbay, Image structure representation and processing: a discussion of some segmentation methods in cytology, IEEE Trans. Pattern Anal. Mach. Intell. 8 (1986) 140–146.
[6] J.K. Udupa, V.G. Ajjanagadde, Boundary and object labelling in three dimensional images, Comput. Vision Graphics Image Process. : Image Understanding 3 (1990) 355–369.
[7] L. Thurfjell, E. Bengtson, B. Nordin, A new three-dimensional connected component labelling algorithm with simultaneous object feature extraction capability, Graphical Models Image Understanding 54 (1992) 357–364.
[8] R. Jain, R. Kasturi, B.G. Schunk, Machine Vision, McGrawhill Inc., New York, 1995.
[9] F. Cheevasuvit, H. Maitre Vidal-Madjar, A robust method for picture segmentation based on split-and-merge procedure, Computer Vision Graphics Image Processing 34 (1986) 268–281.
[10] S. Zucker, Region growing: childhood and adolescence, Comput. Graphics Image Process. 5 (1976) 382–399.
[11] R. Kohler, A segmentation system based on thresholding, Comput. Graphics Image Process. 15 (1981) 319–338.
[12] S. Beucher, The watershed transformation applied to image segmentation, Scanning Microsc. 6 (1992) 299–314.
[13] S. Beucher, F. Meyer, The morphological approach to segmentation: the watershed transformation, in: E.R. Dougherty (Eds.), Mathematical Morphology in Image Processing, Moreel Deckker Inc., New York, 1993.
[14] L. Vincent, Morphological grey scale reconstruction in image analysis: Applications and efficient algorithms, IEEE Trans. Image Process. 2 (1993) 176–201.
[15] S.J. Lockett, B. Herman, Automatic detection of clustered fluorescent stained nuclei by digital image based cytometry, Cytometry 17 (1994) 1–12.
[16] L. Najman, M. Schmitt, Geodesic Saliency of watershed contours and hierarchical segmentation, IEEE Trans. Pattern Anal. Mach. Intell. 18 (1996) 1163–1173.
[17] N. Malpica, C.O. Solorzano, J.J. Vaquero, A. Santos, I. Vallcobra, J.M.G. Sagredo, F. del-Pozo, Applying watershed algorithms to segmentation of clustered nuclei, Cytometry 28 (1997) 289–297.
[18] P.K. Sahoo, S. Soltani, A.K.C. Wong, Y.C. Chen, A survey of thresholding techniques, Computer Vision Graphics and Image Processing 41 (1988) 233–260.
[19] S. Chen, R.S. Jason, G. Marcus, J.W. Sedat, D.A. Agard, The collection processing and display of digital three-dimensional images of biological specimens, in: J. Pawley (Ed.), Handbook of Biological Confocal Microscopy, Plenum Press, New York, 1995, pp. 197–210.
[20] J.C. Russ, Handbook of Biological Confocal Microscopy, CRC Press, New York, 1995.
[21] R.M. Haralick, L. Shapiro, Computer and Robot Vision, Addison-Wesley Publishing Co., New York, 1992, pp. 157–255.
[22] Ch. Lantuejoul, Detection automatique des lignes de defauts dans les systemes eutectiques lamellaires. Rapport interne. Cntre de Morphologie Mathematique Fontainebleau, France, 1978.
[23] S. Beucher, Ch. Lantuejoul, Use of watersheds in contour detection. International. Workshop on Image Processing, CCETT, Rennes, France, 1979.
[24] G. Borgefors, On digital distance transforms in three dimensions, Comput. Vision Graphics Image Process. 64 (1996) 368–376.
[25] J. Serra, Image Analysis, Mathematical Morphology, Vol. 1, Academic Press, New York, 1990.
[26] F. Meyer, A. Van Driel, Automatic screening of papnicolaou stained cervical smears with the T.A.S., Leitz Symposium on Quantitative Morphology and Image Analysis, 1979.

About the Author—P.S. UMESH ADIGA has received his bachelor and master degrees in Electronics engineering from Mysore and Marathwada Universities, respectively. He has submitted his Ph.D. thesis to Indian Statistical Institute and currently working as a postdoctoral research scientist in Oxford University.

About the Author—DR. B.B. CHAUDHURI has received his Ph.D. from IIT Kanpur. At present he is a Professor and head of Computer Vision and Pattern Recognition Unit of Indian Statistical Institute. He has published more than 200 papers in various journals and conferences. His interests include pattern recognition, image processing, fuzzy logic, OCR, etc.